

Supplementary Information

Dual-Active Li||Te-Bi Liquid Metal Batteries with Enhanced Coulombic Efficiency and Cycle Stability

Yewei Guo ^{a, b}, Zehang Li ^a, Qiao Cu ^a, Shaoming Feng ^a, Weixin Zhang ^a, Kangli Wang^{b,c}, Haomiao Li ^{b,c*}, Kai Jiang ^{b,c**}

^a School of Materials Science and Engineering, Huazhong University of Science and Technology, Wuhan, Hubei, China 430074.

^b State Key Laboratory of Advanced Electromagnetic Technology, School of Electrical and Electronic Engineering, Huazhong University of Science and Technology, Wuhan, Hubei, China 430074.

^c Key Laboratory of Image Processing and Intelligent Control, Huazhong University of Science and Technology, Ministry of Education, China

* Corresponding author.

** Corresponding author.

Email: lihm@hust.edu.cn (H. Li), kjiang@hust.edu.cn (K. Jiang)

Experimental Procedures

Preparation of Materials

The Li||Te-Bi liquid metal batteries (LMBs) were assembled using high-purity Li (99.9%, Aladdin), Te (99.99%, Aladdin), and Bi (99.5%, Aladdin) metals. The molten salt electrolyte consisted of a ternary eutectic mixture of LiF-LiCl-LiBr in a molar ratio of 22:31:47. All materials were pretreated to remove impurities. Lithium metal was melted and absorbed into a foam nickel current collector to ensure uniform distribution, while Te and Bi were alloyed in specific molar ratios under controlled heating conditions. The alloyed cathodes were prepared by heating the Te-Bi mixture at 650 °C for 3 hours in an argon-filled glovebox, followed by controlled cooling to avoid volatilization of Te.

Battery Assembly

The battery assembly was conducted in an inert atmosphere using a two-step sealing process. The foam nickel-lithium composite was connected to the stainless-steel lid as the anode, and the alloyed Te-Bi mixture was placed into a graphite crucible as the cathode. The graphite crucible was fitted into a stainless-steel container to prevent corrosion. The electrolyte was added in its molten state at 550 °C to ensure complete wetting of the electrodes. The battery was sealed using laser welding, and the gap between the anode and cathode was maintained at 12.5 mm to optimize ionic transport.

Coulometric Titration

Coulometric titration was performed to investigate the thermodynamic properties and reaction mechanisms of the Li||Te-Bi system. A Li-Al alloy (25 mol% Li) served

as the reference electrode, while a high-purity Li-Al alloy (45 mol% Li) was used as the counter electrode. The working electrodes were Te-Bi alloys with varying compositions. The experiments were conducted in a controlled environment at 520 °C using the LiF-LiCl-LiBr ternary molten salt electrolyte. The titration current was set at ± 63.6 mA (current density: 100 mA cm^{-2}), with each step lasting 1000 s followed by a 1000 s resting period. The potential of the working electrode was measured relative to the reference electrode, and the electrochemical signals were recorded using an electrochemical workstation (AUTOLAB).

Electrochemical Testing

The batteries were tested at a constant operating temperature of 520 °C using a custom-built heating system. Electrochemical performance, including discharge voltage, coulombic efficiency, and cycling stability, was measured using a potentiostat/galvanostat. Constant-current charge-discharge tests were conducted in the voltage range of 0.4–2.0 V. Impedance spectroscopy and cyclic voltammetry were performed to characterize the reaction kinetics and electrode interface behavior.

Structural Characterization

Post-cycling structural analysis of the cathodes was performed using X-ray diffraction (XRD, Empyrean, PANalytical B.V) and X-ray fluorescence (XRF, M4 TORNADO) spectroscopy to identify reaction products and assess compositional changes, and investigate the distribution of Te, Bi, and their lithiation products.

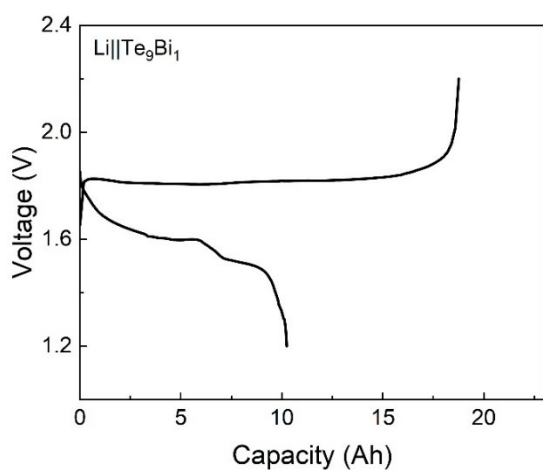


Fig. S1. Charge-discharge curves of Li|LiF-LiBr-LiCl (22:31:47)|Te₉Bi₁

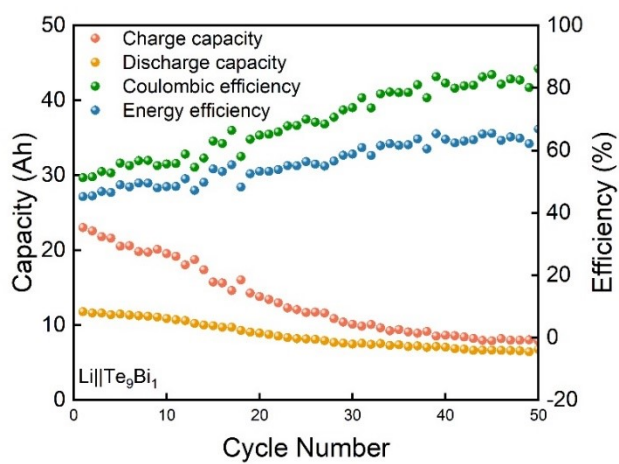


Fig. S2. Cycle performance of Li|LiF-LiBr-LiCl (22:31:47)|Te₉Bi₁

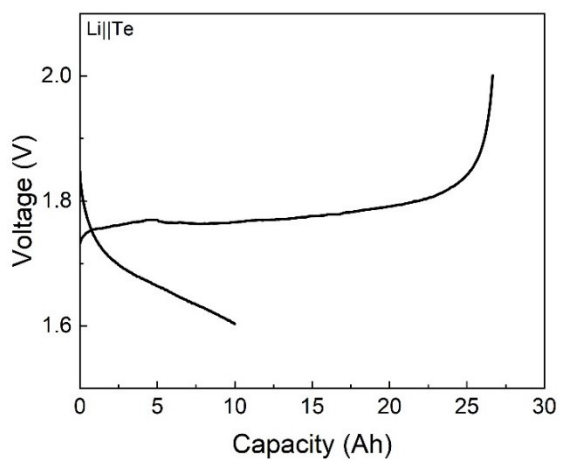


Fig. S3. Charge-discharge curves of Li|LiF-LiBr-LiCl (22:31:47)|Te

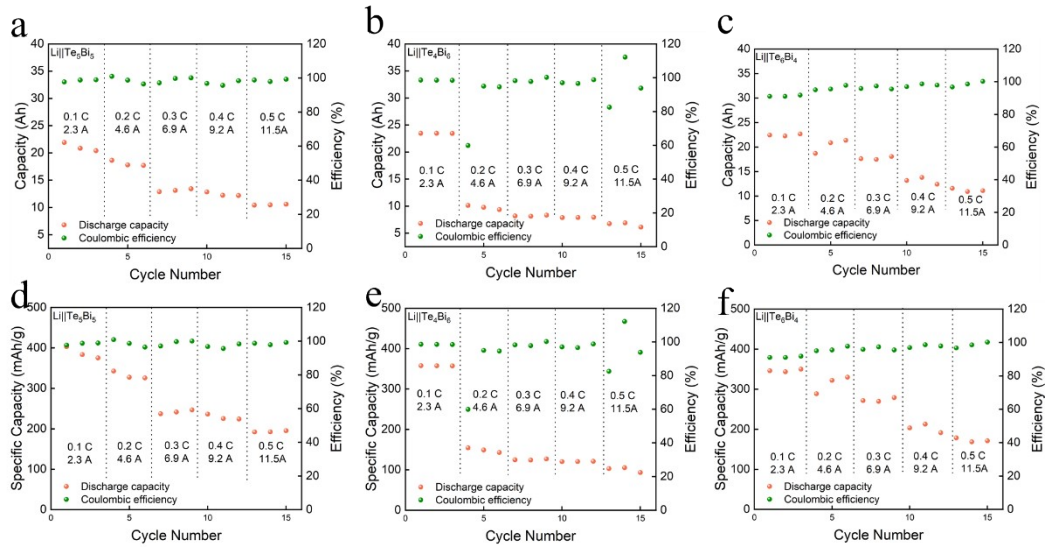


Fig. S4. Rate performance of (a) Li||Te₅Bi₅; (b) Li||Te₄Bi₆; (c) Li||Te₆Bi₄. Corresponding specific capacity curves of (d) Li||Te₅Bi₅; (e) Li||Te₄Bi₆; (f) Li||Te₆Bi₄.

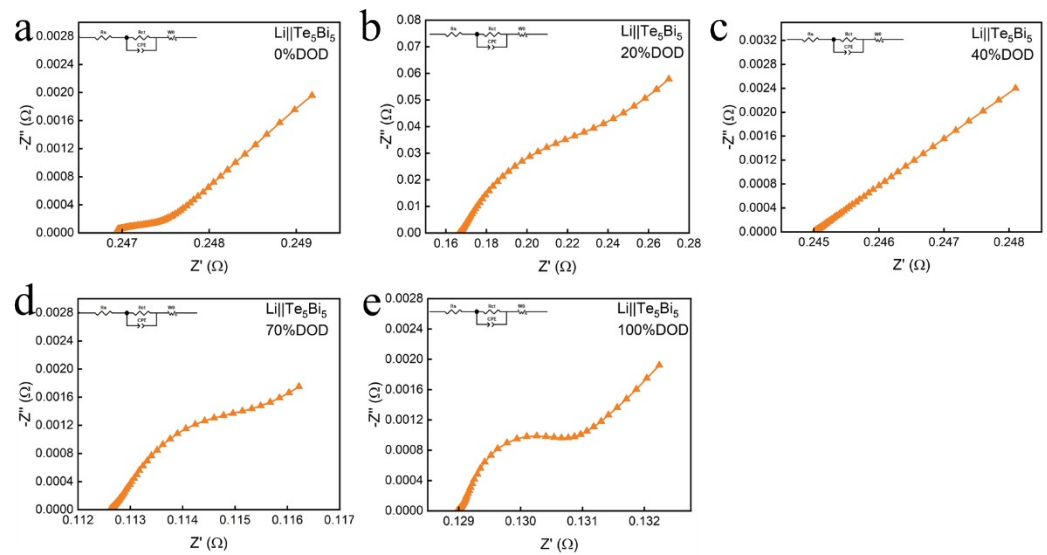


Fig. S5. EIS curves of Li||Te₅Bi₅ at (a) 0%DOD; (b) 20%DOD; (c) 40%DOD; (d) 70%DOD; (e) 100%DOD.

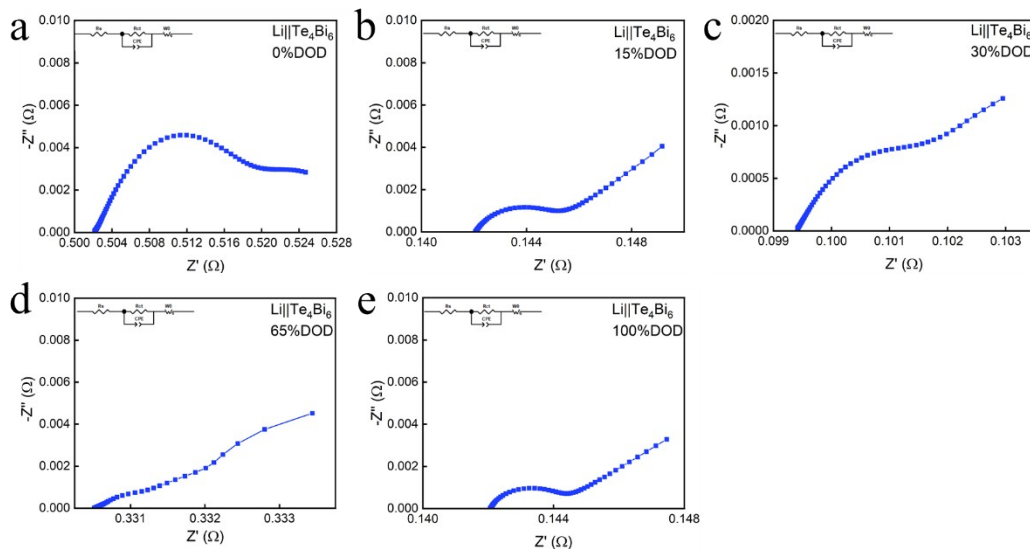


Fig. S6. EIS curves of Li||Te₄Bi₆ at (a) 0%DOD; (b) 15%DOD; (c) 30%DOD; (d) 65%DOD; (e) 100%DOD.

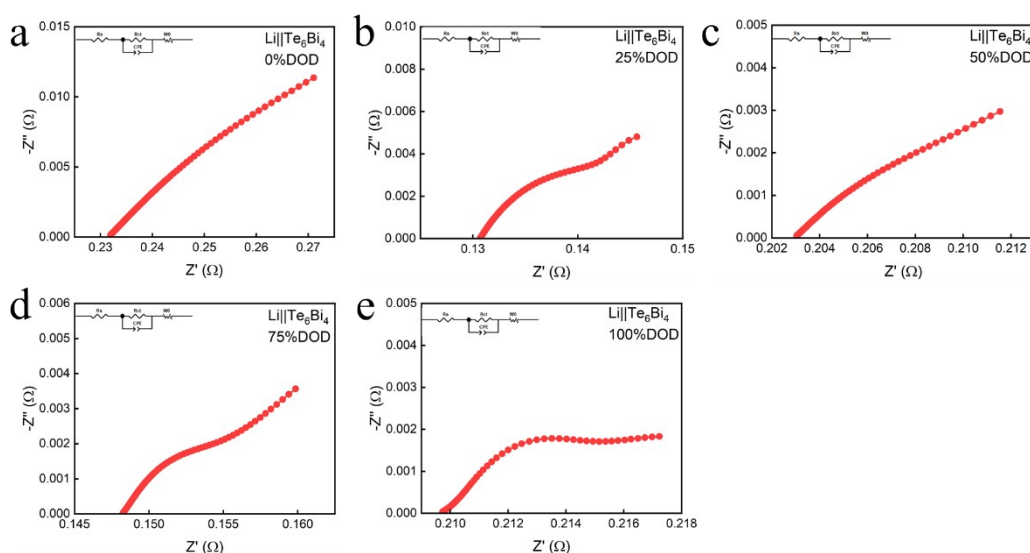


Fig. S7. EIS curves of Li||Te₆Bi₄ at (a) 0%DOD; (b) 25%DOD; (c) 50%DOD; (d) 75%DOD; (e) 100%DOD.

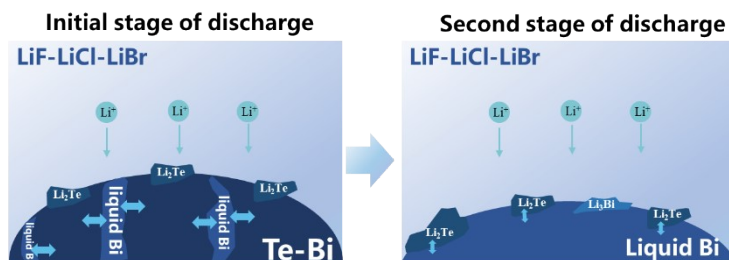


Fig. S8. Reaction Mechanism Schematic of Li||Te₅Bi₅

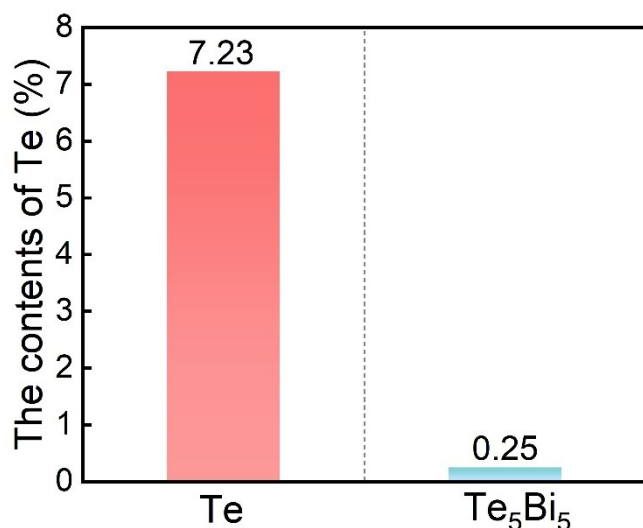


Fig. S9. The contents of Te in the electrolyte at (a) Li||Te and Li||Te₅Bi₅

Table S1. Some parameters of Li||Te₄Bi₆ battery in Figure 2a.

	Li	Bi	Te	Total
Mass/g	6.43	42.32	17.30	65.65
Density/g cm ⁻³	0.534	9.780	6.250	
Amount of substance/mol	0.869	0.203	0.135	
Theoretical capacity/Ah				23.549
Actual capacity/Ah				23.414

Table S2. Some parameters of Li||Te₅Bi₅ battery in Figure 2a.

	Li	Bi	Te	Total
Mass/g	6.17	34.07	20.89	63.74
Density/g cm ⁻³	0.534	9.780	6.250	
Amount of substance/mol	0.889	0.163	0.163	
Theoretical capacity/Ah				23.5033
Actual capacity/Ah				23.256

Table S3. Some parameters of Li||Te₆Bi₄ battery in Figure 2a.

	Li	Bi	Te	Total
Mass/g	6.47	30.42	27.89	64.78
Density/g cm ⁻³	0.534	9.780	6.250	
Amount of substance/mol	0.932	0.146	0.219	

Theoretical capacity/Ah	23.4201
Actual capacity/Ah	23.284

Table S4. Li||Te-Bi Performance comparison with other liquid metal batteries(LMB).

LMB	Capacity(Ah)	Discharge voltage(V)	Energy density(Wh kg ⁻¹)
Li Bi ¹	48.8	0.55	24.6
Li Bi-Pb ²	1.5	0.62	86.0
Li Sb-Sn ³	1.4	0.80	198.3
Li Sb-Pb ⁴	61.8	0.69	103.6
Li Sb-Bi ⁵	2.75	0.70	258.8
Li Sb-Zn ⁶	0.728	0.77	290.6
Li Te-Sn ⁷	2.0	1.50	495.5
Li Te ₅ Bi ₅ (This work)	23.2	0.93	338.9

The energy density (Wh/kg), is calculated based on the Eq. (1):

$$E = \frac{C \times V_{average}}{M} \quad \backslash * \text{ MERGEFORMAT (1)}$$

Where E is the energy density (Wh kg⁻¹); C is the cell capacity (Ah); V_{average} is the average voltage (V); M is the mass of the active materials (kg).

Notes and references

1. X. Ning, S. Phadke, B. Chung, H. Yin, P. Burke and D. R. Sadoway, *Journal of Power Sources*, 2015, **275**, 370-376.
2. J. Kim, D. Shin, Y. Jung, S. M. Hwang, T. Song, Y. Kim and U. Paik, *Journal of Power Sources*, 2018, **377**, 87-92.
3. H. Li, K. Wang, S. Cheng and K. Jiang, *ACS Applied Materials & Interfaces*, 2016, **8**, 12830-12835.
4. K. Wang, K. Jiang, B. Chung, T. Ouchi, P. J. Burke, D. A. Boysen, D. J. Bradwell, H. Kim, U. Muecke and D. R. Sadoway, *Nature*, 2014, **514**, 348-350.
5. T. Dai, Y. Zhao, X.-H. Ning, R. Lakshmi Narayan, J. Li and Z.-w. Shan, *Journal of Power Sources*, 2018, **381**, 38-45.
6. H. Xie, P. Chu, M.-a. Yang, Z. Li, C. Cai, Y. Liu, J. Wang, Z. Fu, Z. Lu, Z. Du and H. Zhao, *Energy Storage Materials*, 2023, **54**, 20-29.
7. H. Li, K. Wang, H. Zhou, X. Guo, S. Cheng and K. Jiang, *Energy Storage Materials*, 2018, **14**, 267-271.